17. P.M. Johansen and O. Breinbjerg, An exact line integral representation of the physical optics scattered field: The case of a perfectly conducting polyhedral structure illuminated by electric Hertzian dipoles, IEEE Trans Antennas Propagat 43 (1996), 689–696.
18. F. Kottler, Electromagnetische theorie der beugung an schwarzen schirmen, Ann Phys 71 (1923), 457–508.
19. F. Kottler, Diffraction at a black screen, Part II: Electromagnetic theory, Progr Opt 6 (1967), 331–377.

MEASUREMENT OF THE TEMPORAL DELAY OF A LIGHT PULSE THROUGH A ONE-DIMENSIONAL PHOTONIC CRYSTAL

Shamino Wang,[1] Hernan Erlig,[1] Harold R. Fetterman,[1] Eli Yablonovitch,[1] Victor Grubsky,[2] Dmitry S. Starodubov,[2] and Jack Feinberg[2]
[1] Department of Electrical Engineering
University of California
Los Angeles, California 90095
[2] Department of Physics
University of Southern California
Los Angeles, California 90089-0484

Received 4 June 1998

ABSTRACT: *We measure a maximum group delay of 22.6 ps for a light pulse propagating through a 1 cm long fiber Bragg grating when the frequency of the light is tuned near the band edge of the grating. Our measurements are performed in the time domain with single picosecond resolution using wavelength-tunable pulses of 0.5 nm bandwidth spectrally sliced from a mode-locked laser. Our experimental results are qualitatively confirmed by our numerical simulations. Promising applications include optical delay elements for phased-array radar and encoders/decoders in spread-spectrum code-division multiple-access systems.* © 1999 John Wiley & Sons, Inc. Microwave Opt Technol Lett 20: 17–21, 1999.

Key words: *group delay; fiber Bragg grating; photonic crystal; wavelength slicing; code-division multiple access*

A one-dimensional photonic crystal is a periodic array of layers with different indexes of refraction. Light propagating at frequencies near the stopband of a photonic crystal will be delayed and dispersed [1], which may prove useful for optically controlled phased-array radars [2]. To date, experimental efforts to measure such delays have been in the frequency domain [3], or in the time domain with a 50 GHz sampling oscilloscope [4]. In this paper, we directly measure the group delay in the time domain with single picosecond resolution, and show that the delay increases as the frequency of the pulse approaches the edge of the photonic crystal's stopband.

We used a Bragg grating in an optical fiber as the one-dimensional photonic crystal. The grating measured ~1 cm in length, had a 1553.20 nm central wavelength, and a 2.10 nm, 3 dB bandwidth. We first theoretically analyzed the physical properties of such a structure using a commercial grating simulation program (IFO_Gratings). To match the actual grating's spectral characteristics, our simulated fiber Bragg grating had a 1 cm long uniform quarter-wave structure and a 0.0035 refractive index change between layers. Figure 1 shows the transmission spectrum and the group velocity as a function of wavelength for the simulated grating. The computed group velocity is seen to drop sharply as the central wavelength of the pulse approaches the edge of the bandgap. Therefore, a tunable delay can be achieved by varying the central wavelength of the propagating pulse with respect to the reflection edge of the grating.

To measure the delay induced by the actual grating, we used the tunable picosecond source shown in Figure 2. The 1.55 μm mode-locked erbium-doped fiber laser emitted a 160 fs (FWHM) pulse train with a 56 nm (FWHM) bandwidth. For the experiments here, we needed a tunable source whose bandwidth was smaller than the width of the grating stopband, which is usually on the order of nanometers. To narrow the frequency spectrum of our pulsed laser, we used an HP 71451B optical spectrum analyzer as a wavelength slicer [5]. By selecting the resolution bandwidth of the spectrum analyzer, we could vary the pulse bandwidth from 0.1 to 10 nm. The pulse center wavelength was tuned by selecting slices of different spectral content. An autocorrelator and a second spectrum analyzer were used to perform diagnostic tests. The results are shown in Figure 3. Note that as the pulse's spectral bandwidth decreased, its temporal length increased, as required by the uncertainty principle.

Light from the wavelength-tunable picosecond source was split into two beams. One beam was sent into the fiber containing a Bragg grating, and the other beam was sent into a reference fiber. The two transmitted signals were recombined and sent to an autocorrelator with a scan window ~120 ps. The autocorrelator displayed both the autocorrelation and the cross-correlation traces. The length of the grating arm was made intentionally longer (by ~1 cm) to separate the autocorrelation and cross-correlation traces (by ~56 ps). Any group delay caused by the fiber Bragg grating produced an additional displacement of the cross-correlation trace relative to the autocorrelation trace. The cross-correlation trace also revealed any dispersion caused by propagation through the grating. Note that any dispersion caused by the fiber itself was common to both pulses.

A typical transmission spectrum of the fiber Bragg grating is shown in Figure 4(a). The spectrum analyzer bandwidth was set to chop 0.5 nm wide wavelength slices; the resulting pulses had a ~16 ps (FWHM) autocorrelation. The chopped slices were not Gaussian, and fitted approximately the sinc-squared function predicted from a "top hat" spectral distribution over the range considered here. Correlation traces were obtained as the pulse's central wavelength was positioned at various wavelengths near the grating bandgap. For trace A in Figure 4(b), we expected and saw no additional delay from the grating. However, the measured group delays for points B, C, and D increased from the 56 ps value by 1.9, 11.4, and 22.6 ps, respectively, as the central wavelength of the pulse approached the edge of the grating's stopband.

From our simulation, we expected the following trends as the laser wavelength neared the grating bandgap: 1) increasing group velocity delay, 2) increasing dispersion, and 3) reduced transmission due to increased reflectivity nearer the grating. Indeed, traces B, C, and D confirm that: 1) the cross-correlation peaks moved further away from the autocorrelation traces, 2) the cross-correlation traces spread out in time due to increased dispersion, and 3) the peak intensities of the cross-correlation traces dropped because of lower transmission as the bandgap was approached. Similar trends were also observed as the bandgap was approached from

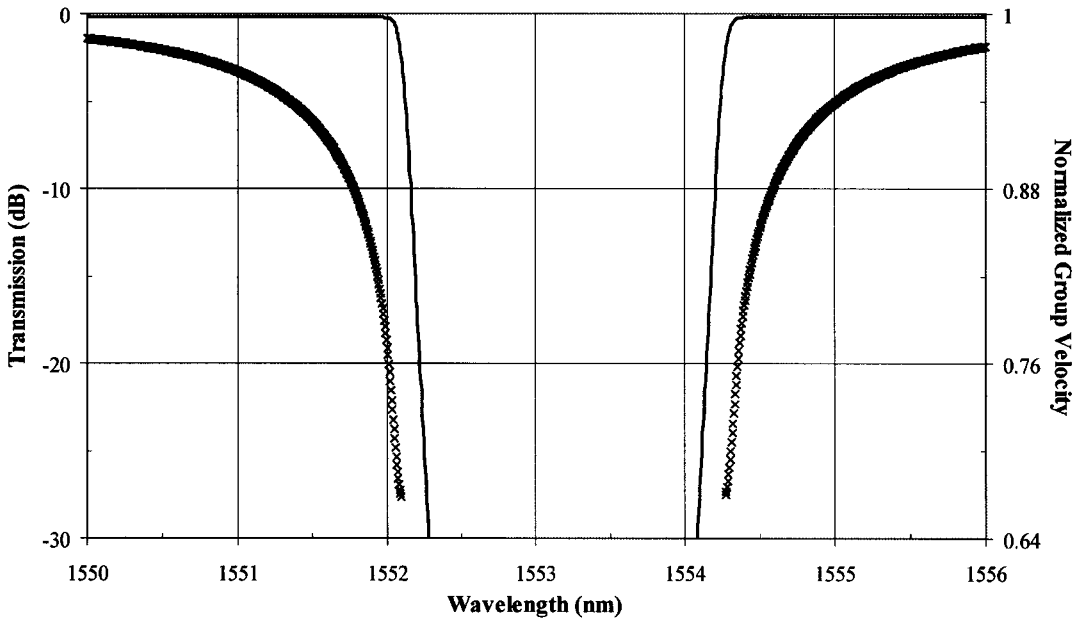

Figure 1 Simulation of a fiber Bragg grating centered at 1553.20 nm with a rectangular index profile. The solid line represents the transmission spectrum and the crosses the group velocities. A refractive index difference between layers of $\Delta n = 0.0035$ was used to match the measured spectrum. The group velocities are normalized to the speed of light in bare fiber

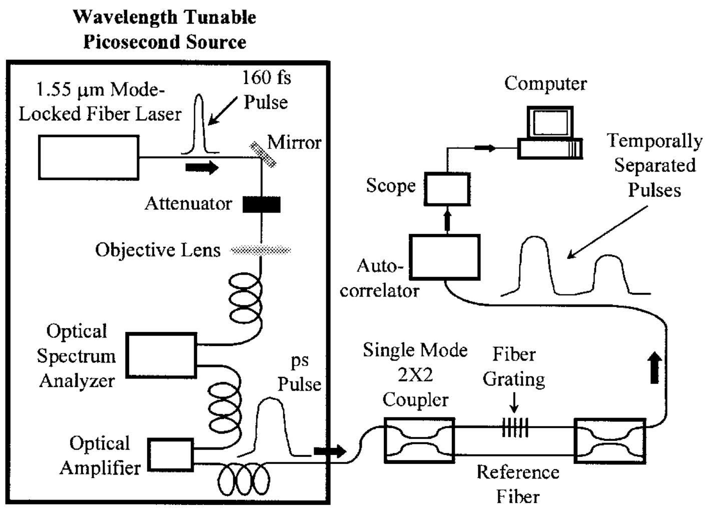

Figure 2 Group delay measurement setup. The autocorrelator displays both the autocorrelation and cross-correlation traces, with the separation between the traces equal to the temporal separation between the reference pulse and the lagging grating pulse

longer wavelengths, as shown in Figure 4(c). The measured additional group delays for points E and F were 8.2 and 3.1 ps, respectively.

Here, we have clearly demonstrated directly in the time domain that a photonic band structure can serve as a delay line in transmission. The 22.6 ps group delay caused by the grating used here corresponded to a 50% increase in the grating's effective length. That is, the 1 cm Bragg grating was equivalent to a 1.5 cm long delay line. We expect longer delays as the grating parameters are optimized in future experiments. One application for such delay lines is in phased-array radar systems, where the conventional chirped gratings and circulators/couplers might be replaced by simple uniform Bragg gratings.

It has also been proposed that photonic bandgap materials could be used as dispersion compensators [3, 6, 7]. By differentiating the group velocity with respect to wavelength, we find negative group velocity dispersion on the short-wavelength side of the grating bandgap and positive group velocity on the long-wavelength side. In principle, we can design a grating pair with different stopband locations such that positive dispersion from the first grating would compensate negative dispersion from the second grating [8]. In addition, one could put a grating in a transmitter and a second conjugate

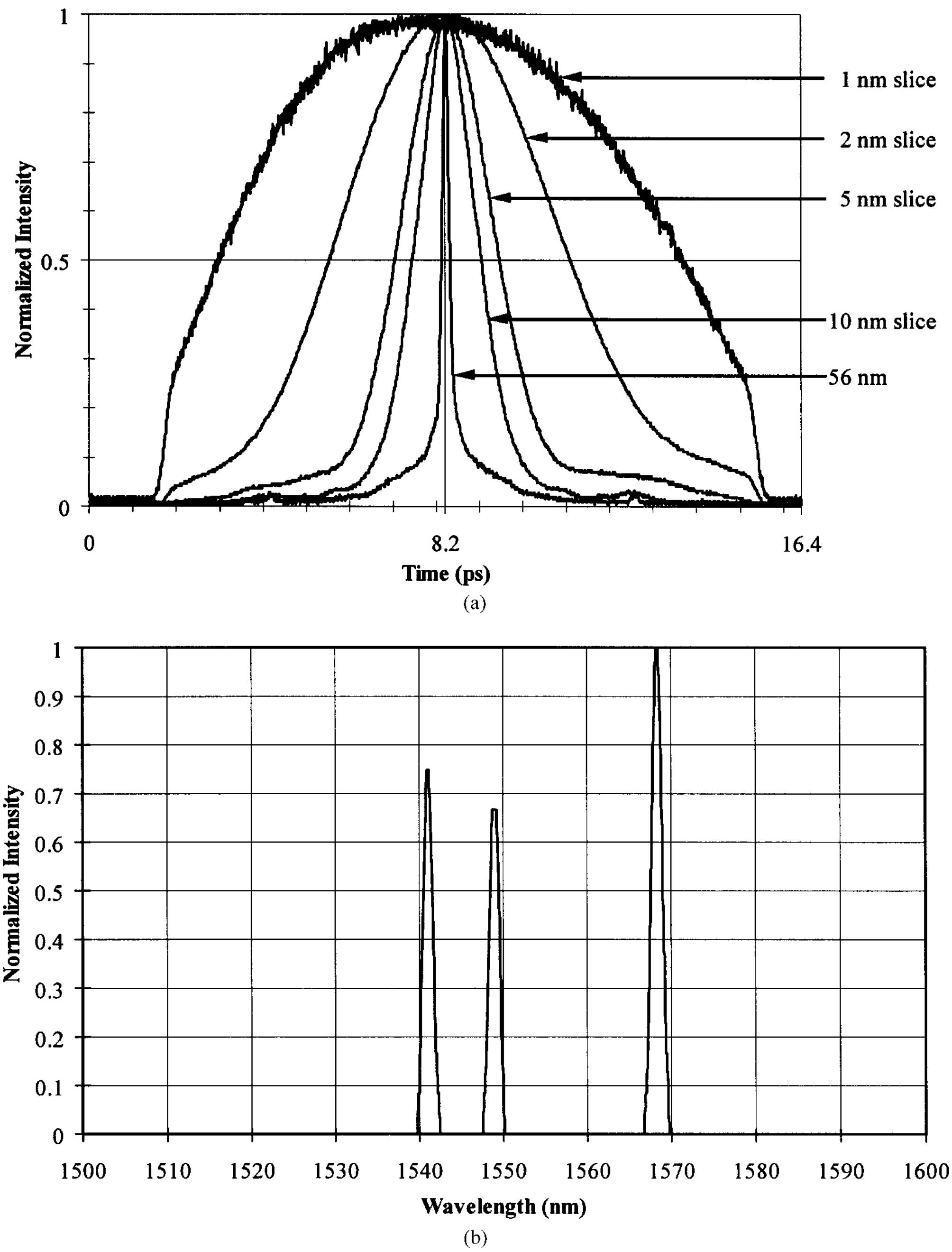

Figure 3 (a) Autocorrelation traces of the 56 nm (FWHM) bandwidth laser pulse and of various wavelength slices. (b) Tunability of a fixed bandwidth slice within the available 56 nm (FWHM) laser bandwidth

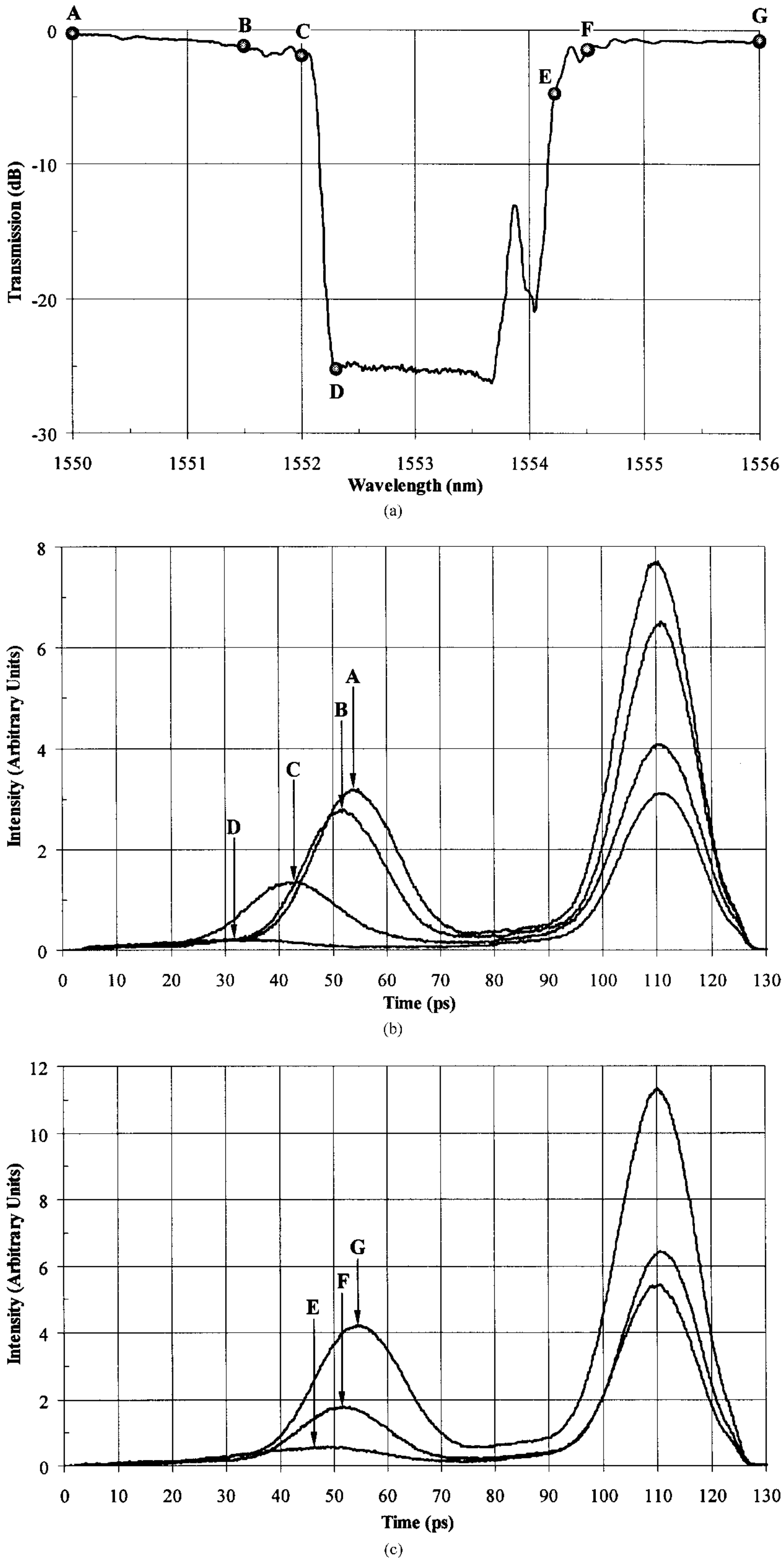

Figure 4 (a) Transmission spectrum of the fiber Bragg grating under test. Operating wavelengths for the points of interest are A: 1550.00 nm, B: 1551.50 nm, C: 1552.00 nm, D: 1552.25 nm, E: 1554.20 nm, F: 1554.50 nm, and G: 1556.00 nm. (b) Correlation traces for points A, B, C, and D. The autocorrelation traces are located at 110 ps. (c) Correlation traces for points E, F, and G. The autocorrelation traces are located at 110 ps

grating in a receiver for use as encoding/decoding components for spread-spectrum code-division multiple-access matched filter systems.

In conclusion, for the first time, to our knowledge, we have measured in the time domain, with single picosecond resolution, the group velocity delay caused by a pulse propagating near the edge of the stopband of a one-dimensional photonic crystal. Such delays can have practical applications for phased-array radar and matched filter systems.

ACKNOWLEDGMENT

This research was supported by the Air Force Office of Scientific Research (AFOSR) and by the Ballistic Missile Defense Organization (BMDO).

REFERENCES

1. M. Scalora, R.J. Flynn, S.B. Reinhardt, R.L. Fork, M.J. Bloemer, M.D. Tocci, C.M. Bowden, H.S. Ledbetter, J.M. Bendickson, J.P. Dowling, and R.P. Leavitt, Ultrashort pulse propagation at the photonic band edge: Large tunable group delay with minimal distortion and loss, Phys Rev E 54 (1996), R1078–R1081.
2. W.H. Loh, R.I. Laming, N. Robinson, A. Cavaciuiti, F. Vaninetti, C.J. Anderson, M.N. Zervas, and M.J. Cole, Dispersion compensation over distances in excess of 500 km for 10-Gb/s systems using chirped fiber gratings, IEEE Photon Technol Lett 8 (1996), 944–946.
3. B.J. Eggleton, T. Stephens, P.A. Krug, G. Dhosi, Z. Brodzeli, and F. Ouellette, Dispersion compensation using a fibre grating in transmission, Electron Lett 32 (1996), 1610–1611.
4. B.J. Eggleton, C.M. de Sterke, and R.E. Slusher, Nonlinear pulse propagation in Bragg gratings, J Opt Soc Amer B 14 (1997), 2980–2993.
5. T.M. Goyette, W. Guo, F.C. De Lucia, J.C. Swartz, H.O. Everitt, B.D. Guenther, and E.R. Brown, Femtosecond demodulation source for high-resolution submillimeter spectroscopy, Appl Phys Lett 67 (1995), 3810–3812.
6. N.M. Litchinitser, B.J. Eggleton, and D.B. Patterson, Fiber Bragg gratings for dispersion compensation in transmission: Theoretical model and design criteria for nearly ideal pulse recompression, J Lightwave Technol 15 (1997), 1303–1313.
7. N.M. Litchinitser and D.B. Patterson, Analysis of fiber Bragg gratings for dispersion compensation in reflective and transmissive geometries, J Lightwave Technol 15 (1997), 1323–1328.
8. S. Wang, H. Erlig, H.R. Feterman, E. Yablonovitch, V. Grubsky, D.S. Starodubov, and J. Feinberg, submitted to IEEE Microwave Guided Wave Lett.

MICROWAVE FREE-ELECTRON LASER WITH AN EXTERNAL ADDITIONAL BACK-COUPLING CIRCUIT

Igor V. Ivanchenko[1]
[1] Institute of Radiophysics & Electronics
National Academy of Sciences of Ukraine
Kharkov 310085, Ukraine

Received 20 May 1998

ABSTRACT: *The spatial amplitude–phase field distributions have been studied in the original electromagnetic structure serving as a waveguide analog of a two-reflector open resonator, with the aid of a new method developed by the author. Such a resonator is used to provide an internal positive back coupling in the microwave oscillator. Analysis and experimental results are given for a microwave free-electron laser (FEL), using the Smith–Purcell effect, with an external additional back-coupling circuit. It has been shown that an external additional back-coupling circuit can be used in this microwave oscillator design without any effect on the matching between the resonance contour and microwave load. This enables one to efficiently control the tube dynamic characteristics and to increase the dynamic system stability to the feeding circuit fluctuations.*

Key words: *millimeter waves; diffraction radiation; open resonator; microwave generator and amplifier; external additional back-coupling circuit*

1. INTRODUCTION

Well-known classical ideas about the properties of the diffraction radiation (DR), also known as the Smith–Purcell effect, emitted when an electron beam moves over a periodic structure, have conditioned the choice of a high Q-factor two-reflector open resonator (OR) as a microwave oscillation contour for medium-power orotron oscillators [1, 2], electron-vacuum microwave amplifiers [2, 3], and transformers [4, 5]. However, even the first experimental investigation of the Smith–Purcell effect in the short-wave part of the millimeter wavelength band led to discovering the detailed spatial structure of the diffraction radiation (DR) [6]. The obtained results have shown an intensive DR at the E-plane normal to the propagation direction of the nonrelativistic electron beam. This formed the basis of DR usage in the new auto-oscillation O-type dynamic devices with extended interaction, a characteristic feature being the presence of nonaxial DR. These devices have been described in detail in [7–9] for the regimes of auto-oscillations, amplification, and chaotic instability. In this paper, the device operation is examined with an external additional back-coupling (EABC) contour both in the auto-oscillation and the oscillation amplification regimes.

2. ELECTROMAGNETIC PROPERTIES OF THE BACK-COUPLING RESONANCE CONTOUR

In Figure 1, a block diagram of the experimental setup for the investigation of the orotron–FEL is shown. The oscillator contour is formed by the lower corner reflector with a diffraction grating (DG) in its central part (the diffraction grating period is 0.4 mm, the length is 32 mm, the width is 10 mm) and the upper plane reflector placed under some angle to the DG plane. In order to obtain maximum usage of the interaction space and the efficient output of the microwave power of the dynamic system, the coupling elements are made as matched pyramidal transitions ending up with the transitions to the waveguides with a standard cross-section 3.6×1.8 mm^2. The resonance contour spectral characteristics were studied in the "cold" regime in [7]. These investigations were carried out for the system excitation applied to both the "input" side of device I (see Fig. 1) and the "output" side of device II. In the first case, the standing-wave coefficient was not more than 2.2, and in the second case, it was increased up to about 3.1.

As one can see from Figure 1, the resonance electromagnetic structure in this device is one of the waveguide analogs of an open resonator (OR). The analysis of the field spatial distributions is necessary to correctly interpret the oscillator properties in different operating regimes. Small geometrical